Extraordinary Lattice Displacement by Pulse Thickness Extension Mode Resonance Oscillation of Acoustic Wave and Its Effect on the Activity for Ethanol Oxidation of a Thin Pd Film Catalyst

H. Nishiyama,† N. Saito, K. Izumi, and Y. Inoue*

Analysis Center, Nagaoka University of Technology, Nagaoka 940-2188, Japan, and Department of Chemistry, Nagaoka University of Technology, Nagaoka 940-2188, Japan

Received: February 5, 2002

Pulse radio frequency (rf) electric power was applied to a ferroelectric single crystal of *z*-cut $LiNbO_3$ to generate pulse thickness extension mode resonance oscillation (p-TERO) of bulk acoustic wave, and the effects of p-TERO on the catalytic activity for ethanol oxidation of a Pd catalyst deposited on the crystal were studied. The employment of the pulse method made it possible to introduce several times larger rf power to the catalyst, compared to conventional continuous rf power introduction. The p-TERO remarkably increased catalytic activity for acetaldehyde production, and its effects were particularly great in a high rf power region. A laser Doppler method was developed to monitor lattice displacement caused by p-TERO. The patterns of lattice displacement became nonuniform in a high rf power region by the appearance of extraordinary lattice displacement. Very large activity increases in the region were associated with the lattice displacement. The mechanism of catalyst activation by p-TERO is discussed.

Introduction

In recent studies of acoustic wave effects on heterogeneous catalysis, the thickness extensional resonance oscillation (TERO) of bulk acoustic waves generated by applying radio frequency (rf) electric power to poled ferroelectric crystals has been proved to have the capability to activate Ag, Pd, and Ni catalysts for alcohol oxidation and decomposition.[1−13] Not only activity but also selectivity has been significantly changed, and it has been suggested that the TERO effects permit the control of heterogeneous catalysis. These findings have shown that TERO has high potential to design a catalyst with artificially controllable functions for chemical reactions, but it is still desired to raise the functions of the TERO effects on catalysis.

For further improvement, one of the useful ways is to introduce as much rf power as possible to catalysts, since the feature of TERO effects is that catalyst activation becomes significantly large in a high rf power region. In addition, a study of catalyst activation in a high power regime will shed a light on the mechanism of acoustic wave excitation. However, there is a limitation that large power introduction frequently gives rise to the crack and break of ferroelectric crystals, and, at most, the largest power employed has been confined to 3 W usually or to 5 W in the successful case.

Continuous rf power introduction has so far been employed, and a practical problem is pointed out that ferroelectric crystals are liable to readily undergo damage under the conditions of large and continuous rf power, in case that impedance deviation occurs even though it is small. In the present study, therefore, a pulse method has been employed: an electric and a catalyst system have been designed to permit the introduction of high rf power. Ethanol oxidation on a Pd catalyst was investigated in the absence and presence of pulse TERO (denoted here as p-TERO), and the results were compared with those previously obtained by continuous TERO (c-TERO).

† Analysis Center.

For measurements of lattice displacement caused by TERO, a homemade laser Doppler apparatus has so far been employed,[7] but it has been found difficult to directly apply it to p-TERO. The apparatus was modified so as to be applicable for p-TERO. Periodic lattice displacement was translated into three-dimensional images.

Experimental Section

A poled ferroelectric single crystal of *z*-cut $LiNbO_3$ (referred to as *z*-LN) with a thickness of 1 mm was cut in a rectangular shape of 14 mm in length and 44 mm in width. A catalytically active Pd film (which also worked as an electrode) was deposited at a thickness of 100 nm on a positively polarized plane of the crystal by resistance-heating of a pure Pd metal in a vacuum, whereas a negatively polarized plane was covered with a catalytically inactive Au (which worked as an electrode only). The catalyst was denoted here as (+)Pd.

Figure 1 shows the diagram of an electric circuit for the generation of p-TERO and a reaction cell. Continuous radio frequency (rf) electric signal from a network analyzer (Anritsu MS3606B) was mixed with a pulse signal from a function generator (Hewlett-Packard, 33120A) and converted to pulse rf signal by a homemade switching device. The pulse rf signal was amplified by an amplifier (ASTECH, AS250FC) and introduced to the catalyst sample after impedance adjustment by a network tuner (Kuranishi, NT-616). The pulse rf power was monitored by a power reflection meter (Rohde & Schwarz, NRT) inserted between the power amplifier and the network tuner. In the present study, the period of switch-on, t_{on}, was equal to that of switching-off time, t_{off}, and the pulse frequency was 3 kHz.

The catalytic ethanol decomposition was carried out in a gas circulating vacuum apparatus, and reactants and products were analyzed by an on-line gas chromatograph. The temperature of catalyst surface was monitored by a noncontacting method using

10.1021/jp0203393 CCC: $22.00
Published on Web 06/04/2002

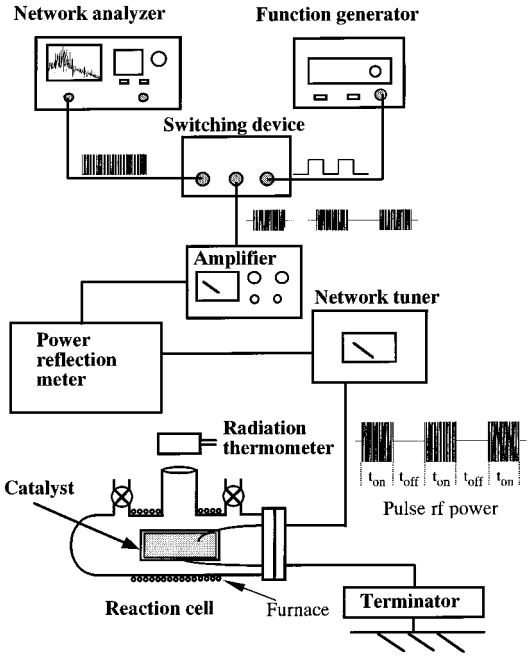

Figure 1. A schematic representation of an electric circuit for the generation of p-TERO and a reaction cell.

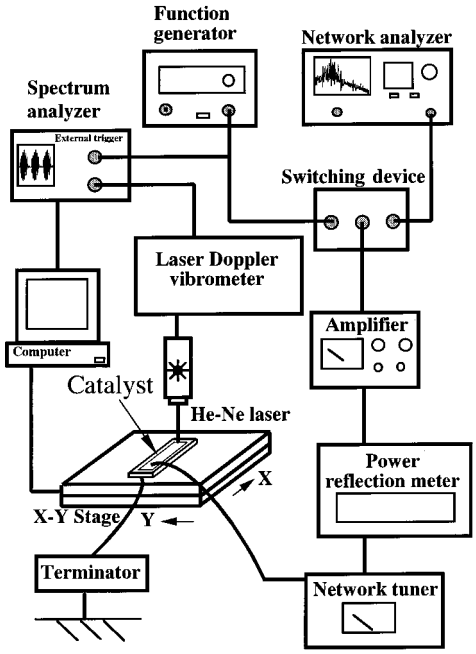

Figure 2. A laser Doppler system for measurements of three-dimensional lattice displacement caused by p-TERO.

a radiation thermometer (Japan Sensor, TME50) through a BaF_2 window of a reaction cell and kept constant by control using an outer electric furnace.

Figure 2 shows a homemade system for measurements of periodic lattice displacement caused by p-TERO. A catalyst surface was irradiated with a He−Ne laser beam, and a reflected beam was analyzed by a vibrometer (Ono Sokki LV-1300) to monitor Doppler shifts. The generation of p-TERO to the surface was carried out in a fashion similar to the method mentioned above. The pulse rf signal produced by the combination of a network analyzer, a function generator and a switching device was amplified and introduced to a catalyst sample after impedance adjustment. A spectrum analyzer (Anritsu MS2651B) was employed in order to synchronize the pulse time by pressing

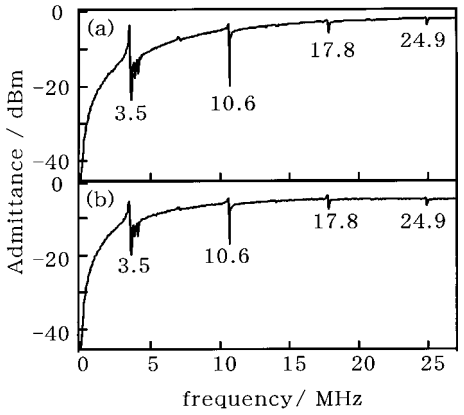

Figure 3. Resonance frequency lines of c-TERO (a) and p-TERO (b).

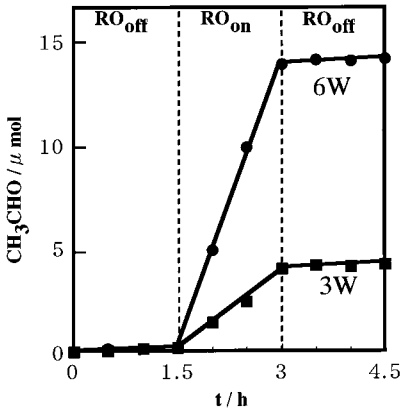

Figure 4. Changes in acetaldehyde production with p-TERO-on and p-TERO-off. ●: 6 W; ■: 3 W. Reaction temperature T_r = 353 K, oxygen pressure = 4.3 kPa, ethanol pressure = 4.3 kPa, pulse frequency = 3 kHz, period of power on = power off = 166 μs.

the trigger on the vibrometer and the function generator. A sample stage was moved along *X* and *Y* direction, while the beam spot was fixed. A whole system was controlled by a computer. A three-dimensional image of *X*−*Y*−*Z* direction was obtained as a pattern, and the distributions of lattice displacement as a function of rf power were obtained.

Results

Figure 3 shows the resonance lines of c- and p-TERO. In c-TERO, the lines appeared at 3.5, 10.6, 17.8, and 24.9 MHz. Exactly the same lines were observed for p-TERO, which intdicates that p-TERO has the same resonance characteristics as observed for c-TERO. The resonance frequency, f_r, for TERO is given, according to a piezoelectric equation,[14,15] by

$$f_r = \{(2n - 1)/2t\}(C_{33}^{E}/\rho)^{1/2}$$

where *n* is 1,2,3, integer, C_{33}^{E} is the elastic constant of a ferroelectric crystal, *t* is thickness of crystal, and ρ is density. The values calculated for *z*-LN and *t* = 1 mm were 3.7, 11.1, 18.4, and 25.8 MHz. The observed frequencies were nearly consistent with the calculated values. The first resonance line of 3.5 MHz was applied for the catalyst activation.

Figure 4 shows ethanol oxidation on a Pd catalyst with p-TERO-off and -on. The production of acetaldehyde increased in near proportion to reaction time. When p-TERO was generated at 3 W, an immediate increase in the production occurred, and the reaction proceeded with a constant enhanced rate. With p-TERO-off, the production decreased to nearly the same low level as before power-on. Activation coefficient, *R*,

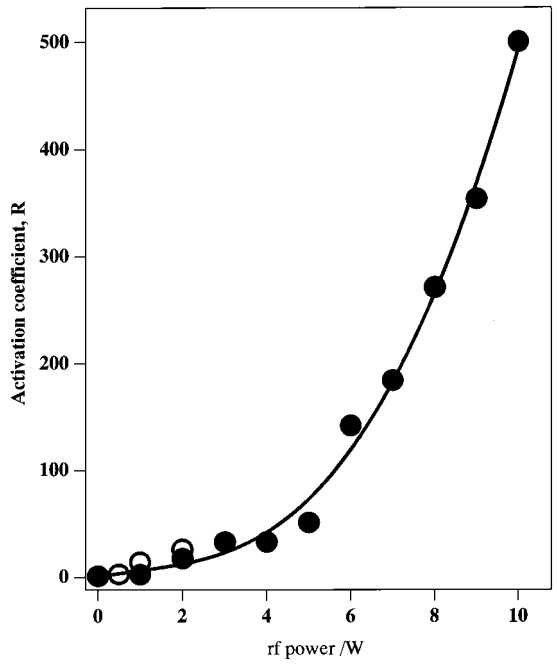

Figure 5. Activation coefficient, *R*, as a function of rf power. ○: continuous rf power; ●: pulse rf power $T_r = 353$ K.

defined as the ratio of activity with p-TERO-on to that with p-TERO-off, was taken as a measure of catalyst activation. At a power of 3 W, the value of *R* was 33. When the power was enhanced to 6 W, an increase in the acetaldehyde production became much larger, and *R* attained at 140.

In the case of p-TERO, the catalytic reaction proceeded under a cycle of power-on and power-off (cf. Figure 1), which means that the catalytic activity observed involves the reaction during the period of power-off. To obtain true catalyst activation by p-TERO, it is necessary to exclude a contribution from the rate for power-off, and the following equation was employed:

$$V_{on} = a^{-1}[(1 + a)\, V_{obs} - V_{off}]$$

where V_{on} is true catalytic activity with power-on, a is the ratio of power-on time (t_{on}) to power-off time (t_{off}), V_{obs} is observed activity, and V_{off} is activity with power-off. In the present case, since $\alpha = 1$ and $V_{obs} > V_{off}$,

$$V_{on} = 2V_{obs}$$

The catalytic activity with p-TERO was obtained according to this equation.

Figure 5 shows changes in catalytic activity for acetaldehyde production as a function of continuous and pulse rf power to generate TERO. With c-TERO, the activity increased gradually up to 2 W. In a lower power region where a gradual increase occurred with increasing pulse power up to 3 W, the activity enhancement with p-TERO was nearly the same as that observed for c-TERO. However, it resulted in a steep rise in a power region larger than 5 W. The activity increased as large as 500-fold by p-TERO at 10 W.

Figure 6 shows the three-dimensional images of lattice vibration caused by p-TERO along the direction vertical to Pd surface. Standing waves appeared randomly over the $X-Y$ planes. The standing wave pattern at a power of 3 W showed the presence of relatively uniform waves and was similar to that observed previously for c-TERO. At 5 W, the standing waves became large, but the uniform standing wave pattern was

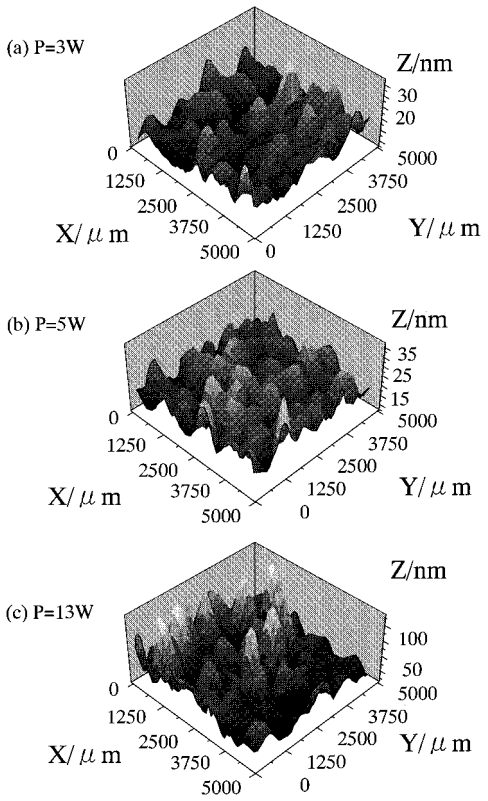

Figure 6. Images of three-dimesional laser Doppler patterns caused by p-TERO. Pulse rf power = (a) 3 W, (b) 5 W, (c) 13 W.

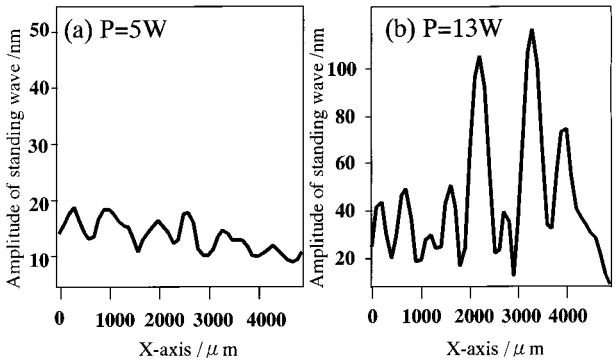

Figure 7. Line profiles of standing waves for p-TERO at (a) 5 W and (b) 13 W.

obtained. At 13 W, however, the pattern changed to involve waves with anomalously large amplitudes and became nonuniform. To clearly see the characteristics of standing waves, Figure 7 shows the line profiles of the waves. Almost all waves had similar amplitudes for p-TERO at 5 W, whereas a part of the waves became extraordinarily large at 13 W, indicating the nonuniformity of the waves.

The amplitude of standing waves corresponds to the magnitude of lattice displacement vertical to the surface. The distributions of lattice displacement were compared for 5 and 13 W. As shown in Figure 8, for p-TERO at 5 W, the distribution peak is narrow, and the lattice displacement was present between 0 and 35 nm. On the other hand, for p-TERO at 13 W, the shape of distribution peak was nonsymmetric and had a long tail toward larger lattice displacement, exhibiting the presence of extraordinarily large lattice displacement: the largest lattice displacement attained at 120 nm.

Figure 9 shows maximum lattice displacement, L_{max}, as a function of pulse rf power. The value of L_{max} increased

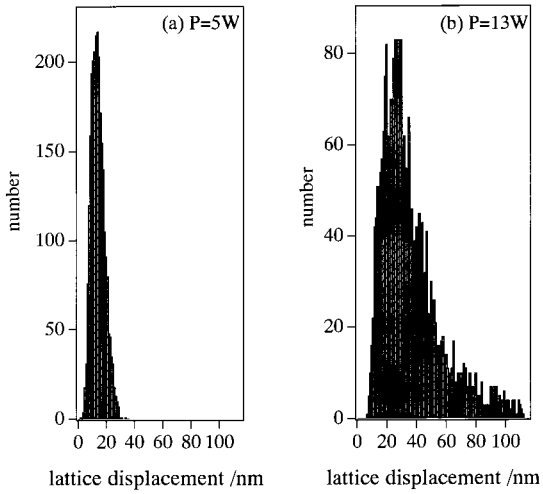

Figure 8. Distributions of lattice displacement for p-TERO at (a) 5 W and (b) 13 W.

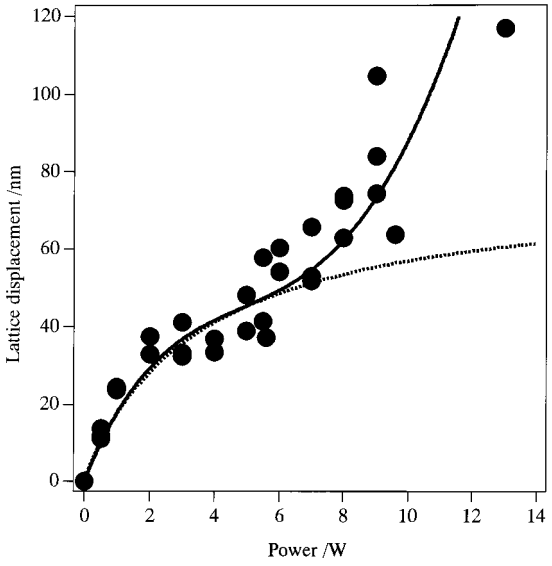

Figure 9. Maximum lattice displacement, L_{max}, as a function of pulse rf power. A dotted line shows a correlation of L_{max} vs square root of rf power.

considerably in a lower power range below 2 W, followed by a gradual enhancement between 2 and 4 W, and a sharp increase above 6 W. The largest L_{max} reached 120 nm at around 10−13 W. The figure also involves a curve (a dotted line) represented by a correlation that the magnitude of lattice displacement increases in proportion to the square root of power.[15] The experimental points were in good agreement with those expected from the equation below 5 W, but exceeded by far the correlation above 6 W. The deviation became larger with increasing rf power.

Figure 10 shows a correlation between activation coefficient, R, and L_{max}. The value of R increased gradually with increasing L_{max} up to 40 nm, followed by a large jump above 50 nm.

Discussion

Pulse rf power with a frequency of 3 kHz provided the same resonance lines as those obtained for continuous power, indicating that TERO was able to stably exist for each period of 166 μs with the same periodicity under the conditions of $\alpha = 1$ and a pulse frequency of 3 kHz. For power introduction, a power of 10−13 W was successfully introduced to a catalyst. Thus,

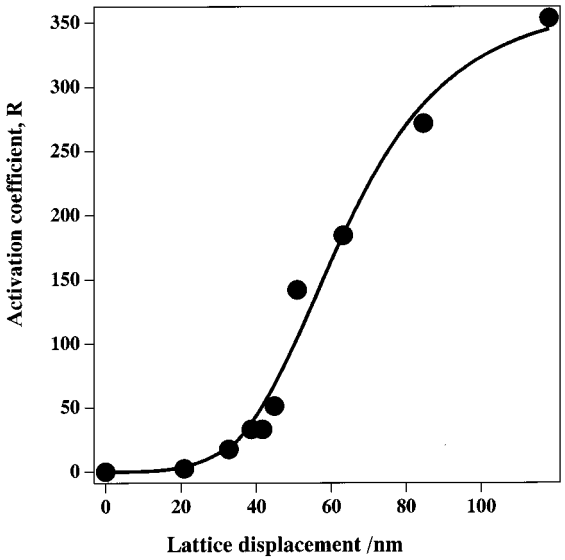

Figure 10. A change in catalyst activation with lattice displacement.

the advantage of the pulse method is that it became possible to introduce approximately 3−4-fold larger power, compared to the conventional continuous method.

As shown in Figure 4, p-TERO caused a remarkable activity enhancement. One might ask that local and short-time thermal effects characteristic of large pulse power would contribute to the enhancement of catalytic activity, even though the entire temperature of a thin film catalyst was controlled. As for heat diffusion in thin metal films, Taketoshi et al. used a picosecond thermoreflectance method and showed that the intensity of thermoreflectance signals for 100 nm Mo and Al films reached saturation within as rapid as 50−100 ps to 100 nm length, indicating that thermal diffusion in the thin films is very fast, and their diffusitivity is close to bulk thermal diffusitivity.[16] In the present study, without temperature control, an increase in catalyst temperature by 5 K was observed by p-TERO at 6 W at 353 K. This obviously indicates that the surface temperature is quickly transferred and can be easily detected by the thermometer. Provided that the activity increase is totally due to thermal effects, calculation using the activation energy of the reaction reported previously[10] leads to a result that a 500-fold activity enhancement could require a temperature rise of 70 K. This temperature rise is high enough to be detected by the thermometer, but the catalytic reaction was examined under the conditions of little increases in temperature with p-TERO-on.

As shown in Figure 6, the three-dimensional images exhibited vertical standing waves that were distributed randomly over the Pd surface. A pattern at 3 W was composed of relatively uniform waves and nearly the same as that previously obtained for c-TERO. The features remained nearly unchanged with p-TERO at 5 W. A correlation of lattice displacement with rf power is usually expressed by a distortion equation that lattice displacement is proportional to the square root of rf power.[15] In the plot of L_{max} vs rf power, the correlation is true below 5 W, but positive deviations occurred above 6 W and became larger with increasing rf power, as shown in Figure 9. For p-TERO at 13 W, standing waves appeared nonuniformly, and the distributions of lattice displacement were extremely nonsymmetric, exhibiting the presence of extraordinarily large lattice displacement. Thus, it is apparent that the deviation from the correlation is related to the presence of extraordinarily large lattice displacement, since the distortion equation assumes uniform distributions of

lattice displacement. These results are indicative of intrinsic differences in lattice displacement between below and above 5 W.

As shown in Figure 10, a correlation between the activation coefficient R and L_{max} gives two distinct regimes: one is a small L_{max} (below 40 nm) region where a gradual increase in the catalytic activity takes place, and the other is a high L_{max} (above 50 nm) region where remarkable enhancement in the activity is induced. It should be noted that in the former the activity enhancement is nearly the same as that for c-TERO, and, furthermore, the lattice displacement with relatively uniform patterns is similar to that observed for c-TERO. On the other hand, the latter corresponds to a region where lattice displacement deviates from the correlation of the distortion equation. Thus, it is evident that the remarkable activity enhancement is brought about by extraordinarily large lattice displacement.

The large lattice displacement is considered to have significant effects on the geometric and electronic structures of the catalyst surface. As the geometric factor, the atom−atom distance and the local geometry of the catalyst surface are considered to vary with periodic lattice displacement. Recently, in self-consistent density function calculations, Mavrikakis et al. demonstrated that strained metal surfaces had chemical properties different from those of unstrained surfaces, and surface reactivity increased with lattice expansion.[17] For example, the CO dissociation barrier of the Ru(0001) plane decreased from 0.8 to 0.6 eV when the surface lattice constant expanded by 1.5%. The largest vertical lattice displacement at 13 W caused the vertical distortion of the order of 10^{-4}% and an increase in the surface atom−atom distance by the order of 10^{-5}%. The latter was obtained by taking L_{max} and the wavelength of wave into account under the assumption of uniform lattice atom expansion. This indicates that the effects of TERO-induced lattice expansion on catalytic activity are negligible. However, the assumption was not true for real lattice displacement, and for more accurate estimation, we need to improve the space resolution of lattice displacement along the *X*- or *Y*-direction. In addition, the possibility is not excluded that specific imperfect sites such as vacancies and dislocations have large effects upon lattice expansion and contribute as a TERO-activated geometric factor to catalyst activation.

For the electronic factor, changes in the electron density are important. In the photoelectron emission spectra, c-TERO caused the shift of threshold energy for electron emission from (+)Pd surface toward higher photon energy, and the magnitudes of shift increased with increasing lattice displacement.[13] The positive shifts were associated with the increases in work function, according to a jellium model.[18,19] Since a large work function has a low ability on the transfer of electrons to the adsorbed species,[20,21] it is thought that an increase in work function converts strongly adsorbed species to weakly adsorbed one. In fact, as shown in a previous study of ethanol oxidation on (+)Pd,[10] c-TERO increased the reaction order with respect to ethanol pressure from 0.2 to 1.0 and decreased the order with respect to oxygen pressure from 0.5 to −0.1. These opposite changes in respective reaction orders indicate that the TERO weakens the adsorption of ethanol and strengthens that of oxygen, which promotes the role of the surface oxygen responsible for the catalytic oxidation, leading to large catalytic activity. From the fact that the work function of the (+)Pd surface increases with increasing lattice displacement, it is readily understood that p-TERO-induced extraordinarily large lattice displacement has quite large effects on catalyst activation.

In conclusion, it is possible to generate large TERO on the catalyst phase by the pulse method and to cause remarkable effects on catalyst activation. The extraordinary lattice displacement is induced by high rf power, which is responsible for a remarkable catalytic activity enhancement. Thus, the combination of acoustic waves with a pulse method is promising in the design of a heterogeneous catalyst with artificially controllable functions.

Acknowledgment. This work was supported by a Grant-in-Aid for Scientific Research (B) from The Ministry of Education, Science, Sports and Culture.

References and Notes

(1) Saito, N.; Inoue, Y. *J. Chem. Phys.* **2000**, *113*, 469.
(2) Inoue, Y. *Catalysis Survey from Japan* **1999**, *3* , 95.
(3) Ohkawara, Y.; Saito, N.; Inoue, Y. *Surf. Sci.* **1996**, 357/358, 777.
(4) Nishiyama, H.; Saito, N.; Shima, M.; Watanabe, Y.; Inoue, Y. *Faraday Discuss.* **1997**, *107*, 425.
(5) Ohkawara, Y.; Saito, N.; Inoue, Y. *Chem. Phys. Lett.* **1998**, *286*, 502.
(6) Saito, N.; Ohkawara, Y.; Sato, K.; Inoue, Y. *MRS Symp. Proc.* **1998**, *497*, 215.
(7) Saito, N.; Nishiyama, H.; Sato, K.; Inoue, Y. *Chem. Phys. Lett.* **1998**, *297*, 72.
(8) Saito, N.; Nishiyama, H.; Sato, K.; Inoue, Y. *Surf. Sci.* **2000**, *454/456*, 1099.
(9) Saito, N.; Nishiyama, H.; Inoue, Y. *Appl. Surf. Sci.* **2001**, *169/170*, 259.
(10) Saito, N.; Sato, K.; Inoue, Y. *Surf. Sci.* **1998**, *417*, 384.
(11) Saito, N.; Ohkawara, Y.; Watanabe, Y.; Inoue, Y. *Appl. Surf. Sci.* **1997**, *121/122*, 343.
(12) Ohkawara, Y.; Saito, N.; Inoue, Y. *Solid State Ionics* **2000**, *136/137*, 819.
(13) Yukawa, Y.; Saito, N.; Nishiyama, H.; Inoue, Y. *J. Phys. Chem.*, submitted.
(14) Ikeda, T. *Fundamentals of Piezoelectricity*; Oxford University Press: New York, 1990; p 117.
(15) Auld, B. A. *Acoustic Fields and Waves in Solids*; Wiley: New York, 1973; Vol. 2.
(16) Taketoshi, N.; Baba, T.; Ono, A. *Jpn. J. Appl. Phys.* **1999**, *38*, L1268.
(17) Mavrikakis, M.; Hammer, B.; Nørskov, J. K. *Phys. Rev. Lett.* **1998**, *81*, 2819.
(18) Lang, N. D.; Kohn, W. *Phys. Rev.* **1970**, *B1*, 4555.
(19) Smith, J. R. *Phys. Rev.* **1969**, 181, 522.
(20) Marcel, R. I. *Principles of Adsorption and Reactions on Solid Surfaces*; Wiley: New York, 1996.
(21) Somorjai, G. *Introduction to Surface Chemistry and Catalysis*; Wiley: New York, 1994.